

HETEROCYCLES, Vol. 72, 2007, pp. 469 - 495. © The Japan Institute of Heterocyclic Chemistry
Received, 4th December, 2006, Accepted, 18th January, 2007, Published online, 19th January, 2006. COM-06-S(K)40

**NMR DETECTION OF INTRAMOLECULAR OH/OH HYDROGEN
BOND NETWORKS: AN APPROACH USING ISOTOPIC
PERTURBATION AND HYDROGEN BOND MEDIATED OH...OH
J-COUPLING**

Carolyn E. Anderson, Alexander J. Pickrell, Sarah L. Sperry, Thomas E. Vasquez, Jr., Thomas G. Custer, Matthew B. Fierman, Daniel C. Lazar, Zachary W. Brown, Wendy S. Iskenderian, Daniel D. Hickstein, and Daniel J. O'Leary*

Department of Chemistry, Pomona College, 645 North College Avenue,
Claremont, California, 91711, USA doleary@pomona.edu

Abstract – A series of conformationally restricted triol and tetrol systems containing intramolecular hydrogen bond arrays has been prepared and characterized by X-ray crystallography and NMR spectroscopy. NMR isotopic perturbation measurements in DMSO-*d*₆ and CD₂Cl₂ reveal that this methodology can be used to detect the spatial proximity of up to four contiguous hydroxyl groups sharing a 1,3-, 1,4-, or 1,5- relationship. Furthermore, hydrogen bond mediated scalar couplings can be used to assign the identity of NMR resonances arising from perturbed OH signals. Our studies suggest that isotope shifts in OH...OH networks are additive. An application in the area of natural product structure elucidation is presented.

INTRODUCTION

It is well-known from solid state studies that intra- and intermolecular arrays of hydroxyl groups can form continuous and cooperative hydrogen bond networks.¹ Intramolecular OH/OH networks also have relevance in discussions of the solution conformational behavior of carbohydrates and natural products, especially those containing polyacetate and polypropionate motifs (Figure 1). Systems with strong intramolecular OH/OH hydrogen bonds have also emerged as a promising class of functional organocatalysts.² The focus of this paper is a description of new NMR methodology for detecting networks of intramolecular OH/OH hydrogen bonds for hydroxyl-containing systems in solution.

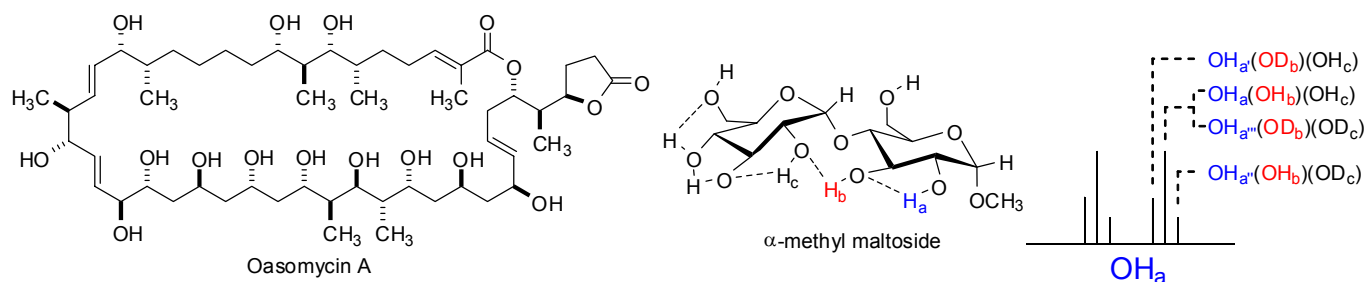


Figure 1. Left: Oasomycin A, a protoypical natural product containing polyacetate and polypropionate motifs. Right: Hydrogen bonding network in α -methyl maltoside in DMSO- d_6 as suggested in Ref. 12. A line spectrum represents the experimental ^1H NMR spectrum of OH_a when the compound is partially deuterated; three chemical shifts (one doublet each for OH_a' , $\text{OH}_a/\text{OH}_a''$, and OH_a''') are thought to arise from each of four isotopically labeled species. That the OH_a chemical shift was sensitive to deuteration at OH_c was taken as evidence of an interresidue hydrogen bond.

Intramolecular hydrogen bonds can be detected with isotope shifts in the ^1H or ^{13}C NMR spectra of partially deuterated compounds, a method referred to as SIMPLE (Secondary Isotope Multiplets of Partially Labeled Entities) NMR.³ Work from our laboratory has explored the origin of this isotope effect in diols, which arises from an isotopic perturbation of equilibrium⁴ involving the intramolecular hydrogen bond (Figure 2).⁵ In particular, we have examined the effects of diol structure and solvent.^{6,7} These studies led to the development of a new ^1H NMR method for assigning the relative configuration of acyclic 1,3-diols typically found in polyacetates and polypropionates.⁸ In related work, we have demonstrated that hydrogen bond mediated OH/OH scalar couplings can be used to detect spatially proximal OH groups in cyclic and acyclic diol systems (Figure 2).^{9,10,11}

In a 1987 report, Christofides and Davies showed that proton SIMPLE NMR measurements were not limited to pair-wise OH interactions and that this method could detect weak and transient OH hydrogen bond networks in molecules such as α -methyl maltoside (Figure 1).¹² The authors showed that in DMSO- d_6 , carbohydrates containing partially deuterated hydroxyl groups gave rise to multiple ^1H resonances for certain OH groups thought to be involved in intramolecular hydrogen bond networks containing as many as three contiguous OH groups. The isotope shifts in these systems tended to be quite small (2-14 ppb), which made their interpretation difficult. Despite these challenges, the authors convincingly demonstrated the detection of several hydrogen bond networks containing three intra-residue and inter-residue OH groups, including the example shown in Figure 1. Importantly, this paper concluded that measurements of very weak intramolecular hydrogen bond networks could be made even in the presence of relatively strong intermolecular hydrogen bonding interactions with solvent molecules. Although the use of DMSO as a solvent for biomolecular structural studies can be criticized for its non-aqueous character, it remains an important medium for studies of carbohydrates. This is due

to its solvating power and its capacity to slow intermolecular proton exchange among hydroxyl groups, which provides sharp hydroxyl ^1H resonances—a prerequisite for high-resolution NMR studies.

Our previous approach to studying hydrogen bonds using the SIMPLE NMR method was to construct rigidified model compounds with well-defined 1,3- or 1,4-diol motifs. By providing strong intramolecular hydrogen bonds, these model compounds exhibited dramatically larger isotope shifts than those previously observed in carbohydrates and natural products. With larger isotope shifts we were able to ascertain some of the factors responsible for the sign of the isotope shift, which can be positive or negative. For example, the sign of the isotope shift had been erroneously linked with the donor/acceptor nature of individual hydroxyl groups.^{3a-b} Our work with symmetric diols, however, illustrated that sign differences in $\text{DMSO-}d_6$ can arise from other factors, such as the limiting chemical shifts ($\delta\text{OH}_{\text{in}}$ vs. $\delta\text{OH}_{\text{out}}$) and the site preference of deuterium (OD_{in} vs. OD_{out}) (Figure 2).

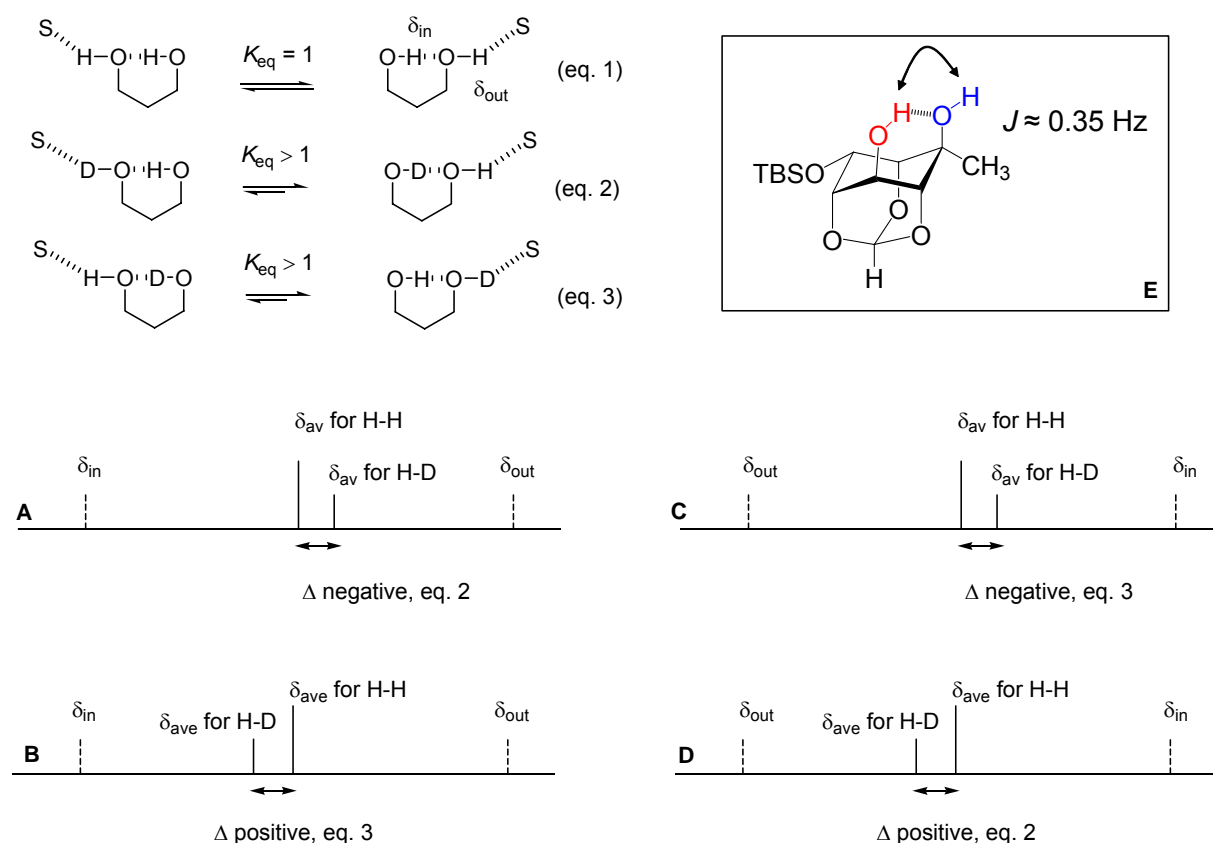


Figure 2. Hypothetical ^1H NMR spectra for hydroxyl groups in a symmetrical diol (eq 1) and unsymmetrical deuterated isotopomers (eqs 2 and 3). (A) A model consistent with upfield (negative) isotope shift associated with deuterium having a preference for the intramolecular hydrogen bond for $\delta_{\text{in}} > \delta_{\text{out}}$ (eq 2). (B) A model consistent with downfield (positive) isotope shift associated with deuterium preferring the intermolecular hydrogen bond for $\delta_{\text{in}} > \delta_{\text{out}}$ (eq 3). (C) A model consistent with upfield (negative) isotope shift associated with deuterium having a preference for the intermolecular hydrogen bond for $\delta_{\text{out}} > \delta_{\text{in}}$ (eq 3). (D) A model consistent with downfield (positive) isotope shift associated with deuterium preferring the intramolecular hydrogen bond for $\delta_{\text{out}} > \delta_{\text{in}}$ (eq 2). (E) An inositol system in which a hydrogen bond mediated scalar coupling between hydroxyl protons is observed (Ref. 9).

The only well-explained systems appear to be those dissolved in apolar solvents such as CD_2Cl_2 or C_6D_6 . In these solvents, $\delta\text{OH}_{\text{in}}$ is reliably downfield of $\delta\text{OH}_{\text{out}}$, and an OD group appears to maintain a preference for the bridging position for reasons related to lowering the zero-point vibrational energy of the system.^{6,13} These two effects conspire to cause the hydroxyl proton of an OH/OD pair to reliably resonate to high field of the parent OH/OH pair (Figure 2C).

Our approach to the study of hydroxyl networks developed as an outgrowth of these investigations with rigid diol systems. We envisioned that SIMPLE NMR measurements using structurally well-defined arrays of hydroxyl groups would allow us to measure isotope effects with “model” hydrogen bond networks. We knew from our earlier investigations that unusually large isotope shifts could be measured in rigid 1,3- and 1,4-diols, and that molecular symmetry could be used to simplify spectra and test hypotheses regarding fundamental aspects of the isotope effect. Therefore, the compounds employed in this study are derivatives of *myo*-inositol monoorthoformate (triol **1** and tetrol **2**) and pentacyclo[5.4.0.02,6.03,10.05,9]-undecane-*endo,endo*-8,11-diol (PCU triol **3** and tetrol **4**). The inositol system provides a contiguous array of 1,3-diols, whereas the PCU system places a 1,4-diol either adjacent to or within a pair of 1,3-diols.

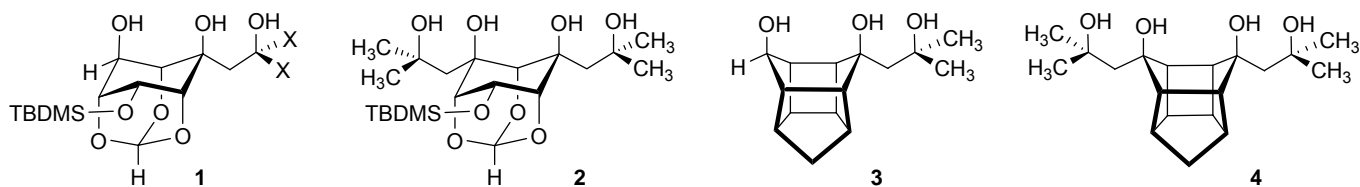


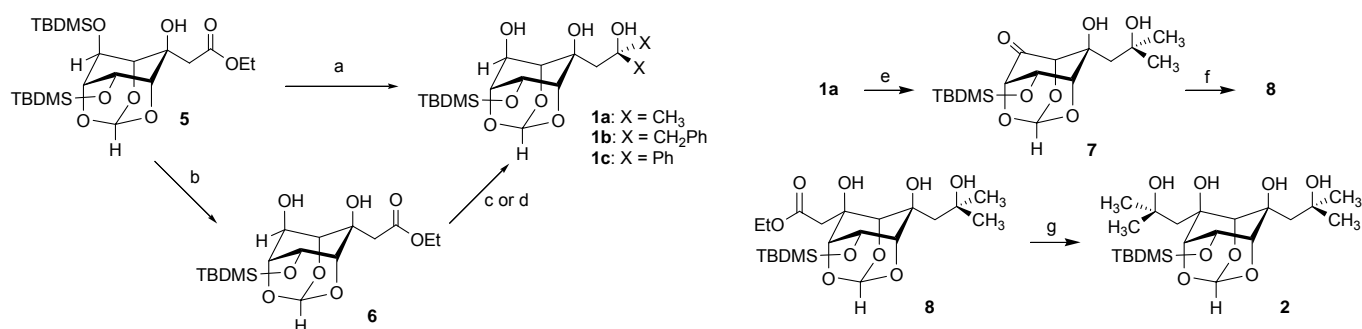
Figure 3. Compounds **1** and **2**: triol and tetrol systems derived from *myo*-inositol monoorthoformate. Compounds **3** and **4**: triol and tetrol systems derived from pentacyclo[5.4.0.02,6.03,10.05,9]-undecane-*endo,endo*-8,11-diol.

With these compounds, we felt that it would be possible to extend Christofides and Davies’ original observations and test the utility of isotopic perturbation to detect networks of intramolecular hydrogen bonds containing up to four OH groups. In the course of our studies on rigid 1,3- and 1,4-diols, we discovered that proximal $\text{OH}\cdots\text{OH}$ spin pairs could be identified through hydrogen bond mediated *J*-coupling (Figure 2). This measurement makes it possible to assign many of the resonances for an isotopically perturbed OH group—something not possible in 1987. These spectra are often complex, and having the ability to fully assign each resonance to a particular isotopolog or isotopomer has provided new insights with respect to the interpretation of these isotope effects in the context of hydrogen bond networks.

RESULTS AND DISCUSSION

Preparation of Inositol-Derived Triol and Tetrol Systems. The synthesis of dimethyl triol **1a** proceeded in a straightforward manner by a room-temperature Grignard addition to ester **5**⁶ (Scheme 1). Under these conditions, the axial OTBDMS silyl ether was observed to quantitatively cleave, thus providing triol array **1a** in one convenient step and 85% yield.

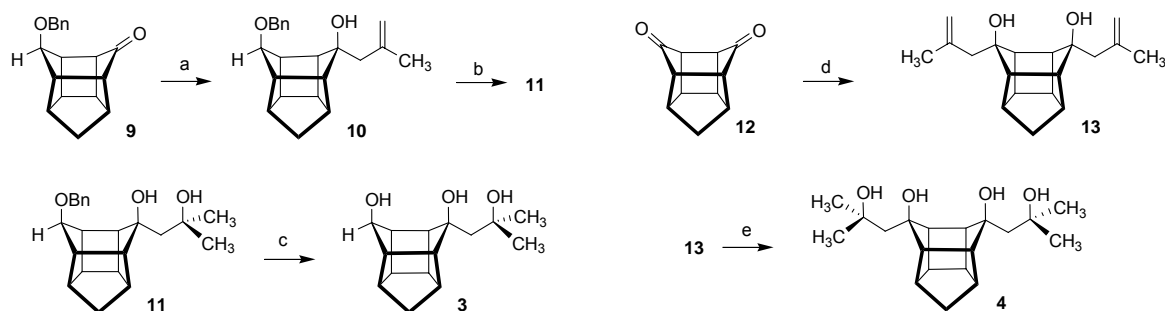
Less basic Grignard reagents, such as benzyl and phenyl magnesium chloride did not, however, remove the axial TBDMS group *in situ*. Rather, this group remained intact and prevented alkylation. This problem was avoided by selective removal of the axial TBDMS group with 1 equivalent of TBAF at low temperature prior to alkylation.⁶ Using this protocol, it was possible to prepare triols **1b** and **1c** from ester **6** in 61% and 89% yield, respectively.



Scheme 1. Reagents and conditions: (a) CH₃MgCl, THF, 0 °C → 25 °C, 85%. (b) 1 eq. TBAF, THF, 0 °C → 25 °C, ref. 6. (c) BnMgCl, THF, rt, 61%. (d) PhMgCl, THF, reflux; isolation; PhMgCl, THF, reflux, 89% (two steps). (e) Dess-Martin periodinane, pyridine/CH₂Cl₂. (f) EtOAc, LiHMDS, THF, -78 °C, 81% (two steps); (g) CH₃MgBr, THF, 0 °C → 25 °C, 69%.

The synthesis of symmetric tetrol **2** commenced with triol **1a**. Oxidation of the secondary alcohol was effected in nearly quantitative yield by use of Dess-Martin periodinane under basic conditions (Scheme 1). The crude ketone **7** was then used directly in a subsequent lithio ethyl acetate addition, providing the ester adduct in 81% yield over the two steps. Conversion to tetrol **2** was then achieved by treatment with methyl Grignard in 69% yield.

Preparation of PCU Triol 3 and Tetrol 4. The synthesis of PCU triol **3** began with known ketone **9**⁹ (Scheme 2). Treatment of ketone **9** with 2-methylallyl magnesium chloride resulted in the formation of tertiary alcohol **10** in 97% yield. Oxymercuration-reduction with mercuric acetate followed by basic sodium borohydride provided diol **11** in 89% yield.¹⁴ Triol **3** was then revealed by removal of the benzyl ether under hydrogenation conditions.



Scheme 2. Reagents and conditions: (a) $\text{CH}_3(\text{CCH}_2)\text{CH}_2\text{MgCl}$, THF, $-78\text{ }^\circ\text{C}$, 97%. (b) $\text{Hg}(\text{OAc})_2$, THF/ H_2O ; NaBH_4 , 3M NaOH, 89%. (c) H_2 (1 atm.), cat. Pd-C, EtOAc, $25\text{ }^\circ\text{C}$, 94%. (d) $\text{CH}_3(\text{CCH}_2)\text{CH}_2\text{MgCl}$, THF, reflux, 98%. (e) $\text{Hg}(\text{OAc})_2$, THF/ H_2O ; NaBH_4 , 3M NaOH, 62%.

Synthesis of the symmetric PCU tetrol **4** proceeded in two steps from commercially available pentacyclo[5.4.0.0.2,6.0.3,10.0.5,9]undecane-8,11-dione (**12**) (Scheme 2). Bisalkylation with 2-methylallyl magnesium chloride provided diene **13** in 98% yield. Subsequent installation of the final two hydroxyl groups was accomplished using a similar oxymercuration-reduction strategy to provide tetrol **4** in 62% yield.¹⁴

X-ray Crystallographic Analyses. The structures of inositol-derived triol **1a** and tetrol **2** as well as PCU-derived arrays **3** and **4** were confirmed by X-ray crystallography (Figure 4).¹⁵ In the crystal structure of triol **1a**, an intramolecular OH/OH hydrogen bond occurs between the diaxial OH groups ($r_{\text{O-O}} = 2.69\text{ \AA}$). The acyclic tertiary hydroxyl group does not form an intramolecular hydrogen bond and is instead rotated away from the diaxial OH/OH pair in order to satisfy an intermolecular hydrogen bond with an acyclic hydroxyl group of an adjacent molecule.

In contrast, the X-ray crystal structure of tetrol **2** shows a contiguous L-shaped intramolecular array of four hydroxyl groups. In the crystal lattice, two molecules align head to tail via two intermolecular hydrogen bonds. This allows for an uninterrupted cyclic array of OH/OH hydrogen bonds. The data suggests that the diaxial hydrogen bond of tetrol **2** is moderately shorter ($r_{\text{O-O}} = 2.66\text{ \AA}$) than in triol **1a**. The external acceptor OH group forms a relatively short intramolecular hydrogen bond ($r_{\text{O-O}} = 2.60\text{ \AA}$), whereas the acyclic donor group is slightly more distal by comparison ($r_{\text{O-O}} = 2.66\text{ \AA}$).

Relative to the OH \cdots OH interactions in **1a** and **2**, the 1,4 diaxial hydroxyl groups in triol **3** and tetrol **4** are in closer proximity to each other, suggestive of a shorter and stronger hydrogen bond ($r_{\text{O-O}} = 2.58\text{ \AA}$ for **3** and $r_{\text{O-O}} = 2.52\text{ \AA}$ for **4**, Figure 4). Interestingly, the O-O distance in diol **13** (X-ray structure not shown)¹⁵ is 2.56 \AA , which suggests that 1,4 OH \cdots OH compression in tetrol **4** might be due to a cooperative hydrogen bonding effect. In triol **3**, the external OH group is a hydrogen bond donor ($r_{\text{O-O}} =$

2.61 Å). Tetrol **4** is similar to tetrol **2** in that the external hydrogen bond donor ($r_{O-O} = 2.62$ Å) is more distal than the external acceptor ($r_{O-O} = 2.56$ Å).

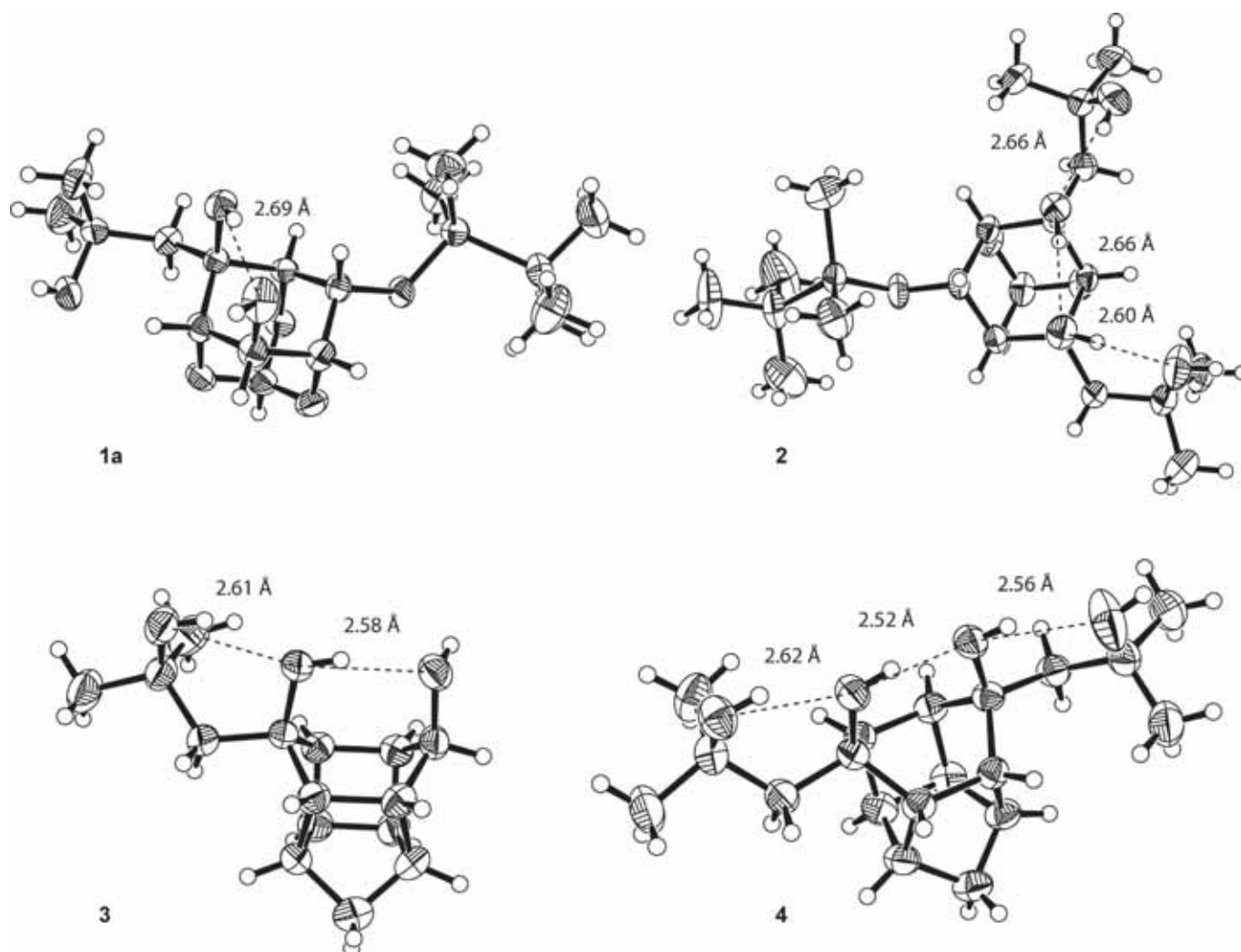


Figure 4. ORTEP plots for triols **1a** and **3** and tetrols **2** and **4**. Oxygen-oxygen distances (r_{O-O} , Å) are shown adjacent to each intramolecular hydrogen bond.

Although it is difficult to ascertain the dependence of these distances upon packing effects, it is worthwhile to note that triol **3** and tetrol **4** possess diaxial OH groups in closest proximity ($r_{O-O} = 2.52$ - 2.58 Å). The acyclic 1,3-diol fragments appear capable of forming reasonably short interactions in all of the compounds, especially when the external OH group acts as a hydrogen bond acceptor ($r_{O-O} = 2.56$ - 2.60 Å). Within the group of molecules studied here, the inositol-derived diaxial 1,3-diols appear to have the weakest OH/OH interactions ($r_{O-O} = 2.66$ - 2.69). Of course, the strength of a hydrogen bond depends on several geometric factors in addition to the oxygen-oxygen distance. Our earlier studies of structurally rigid 1,3- and 1,4-diols suggested that isotopic perturbation measurements in $DMSO-d_6$ were very sensitive to the strength of the intramolecular hydrogen bond: diols possessing short and strong 1,4- hydrogen bonds tended to give negative (upfield) isotope shifts, whereas those with weaker 1,3- hydrogen bonds tended to give positive (downfield) isotope shifts. As mentioned earlier, the sign of the

isotope shift is dependent upon the limiting OH chemical shifts and the site preference of deuterium. A detailed discussion of these factors for systems dissolved in DMSO- d_6 is beyond the scope of this paper. Instead, we present a series of case studies to highlight the application of an operationally simple NMR method for the detection of interacting OH groups.

NMR Hydroxyl Exchange Rate and Temperature Coefficient Studies. OH ^1H resonances are often sharp in DMSO- d_6 because inter- and intramolecular proton exchange is slow in this solvent.¹⁶ We became interested in measuring the exchange rates of the OH groups in several of our molecules in order to see if it would be possible to use this parameter for structural information. We therefore undertook 2D EXSY¹⁷ studies of triols **1a** and **3** at 80 °C; an elevated temperature was necessary to provide a measurable rate of exchange. Proton exchange is highly sensitive to the presence of exchange catalysts, and the relative amount of any such catalysts in our NMR samples could not be controlled for, although care was taken with respect to normalizing solute concentration and water content. This problem with exchange catalysts precludes a direct comparison of rates obtained for triol **1a** with **3**, but it should be valid to compare the relative exchange rates for a given triol.

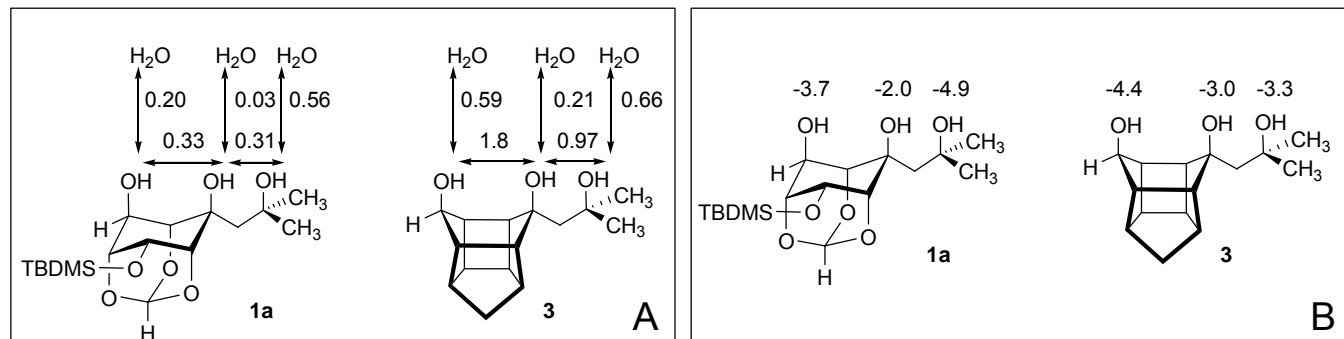


Figure 5. (A) A comparison of magnetization exchange rate constants (s^{-1}) obtained from 2D EXSY spectra for triols **1a** and **3** in DMSO- d_6 at 80 °C. (B) A comparison of OH chemical shift temperature coefficients (ppb K^{-1}) measured in DMSO- d_6 .

The magnetization exchange rate constants for triols **1a** and **3** are shown in Figure 5. In triol **1a**, the rates of 1,3 intramolecular exchange are comparable, whereas the intermolecular exchange rate with water is markedly different for each hydroxyl group. The slowest to exchange with water is the internal OH group, suggesting that this OH group is least accessible. The terminal secondary and terminal tertiary hydroxyl groups exchange with water about six and nineteen times faster, respectively, than the internal hydroxyl group. In triol **3**, the rate of 1,4 intramolecular OH exchange is about twice as fast as the corresponding 1,3 exchange. The relative intermolecular exchange rates in triol **3** are more similar to each other than they were in triol **1a**. The internal tertiary OH exchange rate is still the slowest, however, in triol **3** it was only a factor of three slower than each of the terminal OH groups.

Hydroxyl temperature coefficients in DMSO- d_6 are often used as qualitative indicators of intramolecular hydrogen bonds. Temperature coefficients of -5 to -8 ppb K^{-1} have been used to identify fully solvated OH groups in DMSO- d_6 , whereas coefficients of -1 to -3 ppb K^{-1} are associated with donor hydroxyl groups in strong intramolecular hydrogen bonds.¹⁸ The temperature coefficients in triols **1a** and **3** fall in an intermediate range and span -2.0 to -4.9 ppb K^{-1} .

The magnetization transfer and temperature coefficient experiments provide a measure of the degree of solvent exposure for a given hydroxyl group. Neither experiment provides direct evidence for the spatial proximity of two or more OH groups. On the other hand, the isotopic perturbation and hydrogen bond mediated J -coupling experiments do provide a direct measure of spatially proximal OH groups. The remaining sections of this paper present a series of investigations utilizing this methodology.

NMR Isotopic Perturbation and Hydrogen Bond Mediated J -Coupling Studies. Partial deuteration of the hydroxyl groups in a triol lacking symmetry-related hydroxyl groups can produce up to eight species consisting of two unique isotopomers (OH/OH/OH and OD/OD/OD) and two sets of mono- and dideuterated isotopomers that each contain a subset of three unique isotopologs (Figure 6). We have adopted a labeling system to facilitate a discussion of the hydroxyl groups in these isotopically substituted molecules. Assigning the exocyclic hydroxyl group as C_1 , the carbon chain containing all of the hydroxyl moieties has been numbered. Each enumerated hydroxyl group is then given a letter subscript to assign it to a particular isotopomer or isotopolog. In the case of tetrols containing a mirror plane, the symmetry-related hydroxyl groups are enumerated as X and X' , respectively, with the lettering system retained (Figure 8).

Before the addition of any exchangeable deuterium to a DMSO- d_6 solution of inositol methyl triol **1a**, the 1H NMR spectrum showed three sharp hydroxyl resonances: two singlets corresponding to the tertiary C_1 -OH and C_3 -OH and a doublet corresponding to the secondary C_5 -OH (Figure 6). The downfield singlet was preliminarily assigned to the internal C_3 -OH group on the basis of its relative chemical shift. Upon addition of a sufficient amount of exchangeable deuterium (via microliter titration of CD_3OD), four 1H resonances for each hydroxyl group were observed. As shown in Figure 6, these shifts correspond to the various isotopically labeled species and are reminiscent of Christofides and Davies' 1987 spectra. As these authors pointed out, it is possible to make some signal assignments on the basis of their titration behavior, as peaks corresponding to monodeuterated forms tend to appear first. We note that the spectra in Figure 6 (and throughout this paper) utilize post-acquisition Gaussian resolution enhancement, a

commonly used line-narrowing procedure that provides accurate peak positions, albeit with a small amount of baseline distortion.

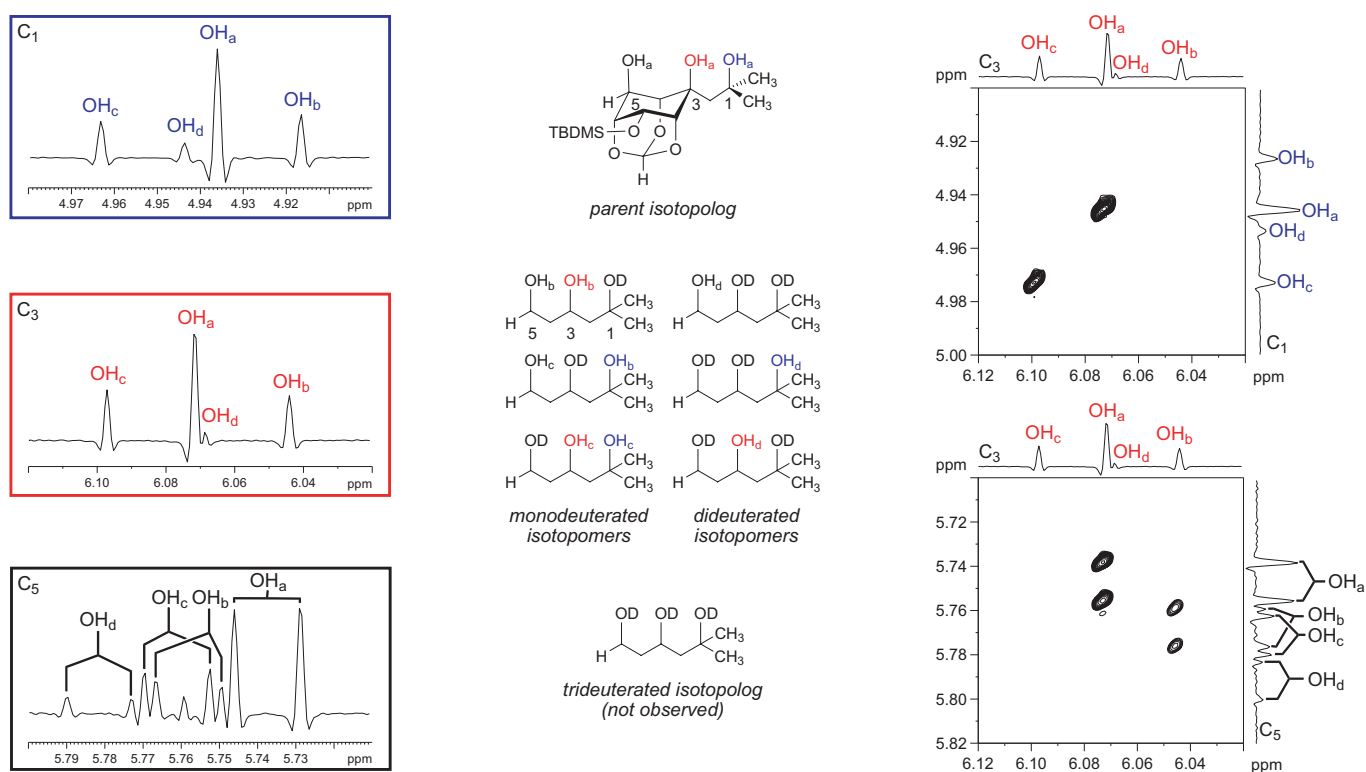


Figure 6. Isotope shift perturbation of triol **1a**. Left: ^1H NMR spectra for each of the three hydroxyl resonances with isotope shifts after partial deuteration of the sample. The isotopically shifted peaks for each hydroxyl group are assigned to their specific hydroxyl proton of the deuterated species shown to the right. These species are represented in simplified form by only the hydroxyl portion of the compound. Right: 2D COSYLR spectra for the partially deuterated triol derivative **1a** with isotope shift assignments (200 ms delay). The region corresponding to C₃-OH/C₁-OH appears at the upper right and that of C₃-OH/C₅-OH is shown at the lower right.

In order to assign each hydroxyl resonance to the corresponding monodeuterated isotopomer, a 2D COSY experiment modified with a refocusing delay (COSYLR) was performed.¹⁹ As described earlier, this experiment detects the $^1\text{H}/^1\text{H}$ coupling between hydroxyl groups sharing a hydrogen bond. We note that for many of the systems presented in this paper, we are using this experiment in a high-resolution manner with a narrow sweep width to optimize digital resolution. This is necessary because the peak separation in isotopically perturbed spectra can be quite small (≈ 1 Hz). The off-diagonal region of the 2D COSYLR spectrum corresponding to C₁-OH and C₃-OH shows two cross-peaks (Figure 6). One cross-peak is due to C₁-OH_a/C₃-OH_a coupling in the parent compound, and the other cross-peak is assigned to C₁-OH_c and C₃-OH_c. The high field C₃-OH resonance also shows a correlation to one of the monodeuterated C₅-OH doublets (Figure 6). This confirms the identity of the C₃-OH_b and C₅-OH_b resonances, as only one monodeuterated isotopomer possesses this pair-wise interaction of OH groups.

With C₁-OH_c, C₃-OH_b, C₃-OH_c, and C₅-OH_b assigned via the COSYLR method, the remaining hydroxyl resonances could be assigned on the basis of their relative intensities. The complete assignments are compiled in Table 1.

Table 1. Isotope shifts (measured and predicted) for triols **1a** and **1b**.

Hydroxyl group	1a : Experimental isotope shift (ppb)	1a : Predicted shift using additivity (ppb)	1b : Experimental isotope shift (ppb)	1b : Predicted shift using additivity (ppb)
C ₁ OH _b (mono)	-19.3		+23.8	
C ₁ OH _c (mono)	+27.0		-12.3	
C ₁ OH _d (di)	+7.8	+7.7 (b+c)	+10.9	+11.5 (b+c)
C ₃ OH _b (mono)	-27.8		-8.6	
C ₃ OH _c (mono)	+25.3		-4.9	
C ₃ OH _d (di)	-3.2	-2.5 (b+c)	-15.0	-13.5 (b+c)
C ₅ OH _b (mono)	+20.5		+20.0	
C ₅ OH _c (mono)	+24.3		+26.3	
C ₅ OH _d (di)	+44.4	+44.8 (b+c)	+45.8	+46.3 (b+c)

The isotope shifts for the hydrogen bonding system in triol **1a** were found to be additive (Table 1). For example, the C₁-OH isotope shifts observed for the monodeuterated isotopomers were -19.3 ppb for C₁-OH_b and +27.0 ppb for C₁-OH_c. Adding these values together results in an isotope shift of +7.7 ppb, a value that compares quite favorably with the observed isotope shift (+7.8 ppb) for C₁-OH_d in the corresponding dideuterated isotopomer. The other two dideuterated isotopomers exhibit similar additivity. To the best of our knowledge, this is the first confirmation of an additive relationship in SIMPLE NMR measurements. As will be shown in later examples, additivity is an extremely useful tool for deconvoluting the often highly complex spectra which arise from partially deuterated tetrols.

Using similar methods of isotopic perturbation and 2D COSYLR experiments, the analogous dibenzyl and diphenyl triols **1b** and **1c**, inositol-derived ester triol **8**, and PCU triol **3** were analyzed. The tabulated results of these studies appear in Tables 1-3 and Figure 7. In each case, isotopically perturbed resonances were assigned utilizing the 2D COSYLR/peak intensity/additivity strategy described for triol **1a**.

The isotope shifts arising from monodeuteration of triols **1a**, **1b**, **1c** and **8** are compiled in Figure 7. We discuss several trends observed for selected OH groups in these compounds. The C₁-OH groups in these

compounds are all tertiary OH groups but their environments differ by virtue of geminal substitution by methyl, phenyl, or benzyl groups. For the case of proximal deuteration, the C₁-OH isotope shifts for Y = Me and Y = Ph are nearly identical but change sign for Y = Bn. When the ester function is present as a putative hydrogen bond acceptor at the network terminus the C₁-OH isotope shifts change sign. We take this latter observation as evidence that the isotopic perturbation method is detecting a contiguous network of OH groups, as the C₁-OH groups in triols **1a** and **8** are in otherwise identical environments with Y = Me. The C₃-OH group shows isotope shifts whose sign largely correlates with deuteration at C₁-OH or C₅-OH; negative isotope shifts are observed when the C₁-OH is deuterated, and positive shifts occur in three cases when the C₅-OH is deuterated. A small negative isotope shift is observed for C₃-OH when the C₅-OH group is deuterated in triol **1b**. As was mentioned earlier, inositol-derived 1,3-diols generally produced positive isotope shifts in DMSO-*d*₆, and diols exhibiting shorter, stronger intramolecular hydrogen bonds generally produced negative isotope shifts. According to the X-ray crystallographic results, the acyclic 1,3-diols form stronger hydrogen bonds than the transannular 1,3-diols on the inositol framework (Figure 4). Although it is clear that exceptions to this rule exist, the interplay of pair-wise intramolecular hydrogen bond strengths appears to be involved in networks that produce monodeuterated isotope shifts of different sign. Consistent with this argument, the C₅-OH monodeuterated isotope shifts are all positive in triols **1a**, **1b**, and **1c**. Interestingly, in **1c**, C₅-OH is much more sensitive to remote deuteration at C₁-OH when Y = Ph: this isotope shift in **1c** is +51.8 ppb, which is 2.5 times larger than the corresponding C₅-OH isotope shift in triols **1a** and **1b**.

Table 2. Isotope shifts (measured and predicted) for diphenyl triol **1c** and ester triol **8**.

Hydroxyl group	1c : Experimental isotope shift (ppb)	1c : Predicted shift using additivity (ppb)	8 : Experimental isotope shift (ppb)	8 : Predicted shift using additivity (ppb)
C ₁ OH _b (mono)	-20.6		-20.4	
C ₁ OH _c (mono)	+28.1		+24.1	
C ₁ OH _d (di)	+7.0	+7.5 (b+c)	+4.7	+3.7 (b+c)
C ₃ OH _b (mono)	-42.4		-36.0	
C ₃ OH _c (mono)	+20.0		+26.8	
C ₃ OH _d (di)	-24.4	-24.4 (b+c)	-9.2	-9.2 (b+c)
C ₅ OH _b (mono)	+51.8		~0	
C ₅ OH _c (mono)	+8.7		+9.3	
C ₅ OH _d (di)	+60.6	+60.5 (b+c)	+9.3	+9.3 (b+c)

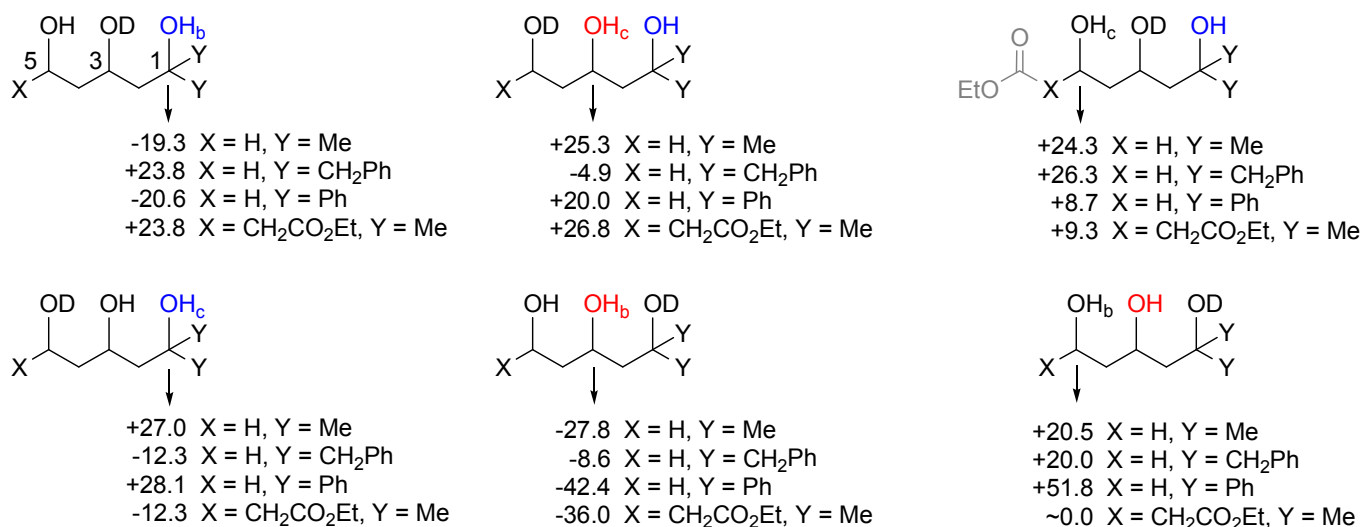


Figure 7. Comparison of isotope shifts (ppb) observed in monodeuterated isotopomers of triols **1a**, **1b**, **1c**, and **8**.

Table 3. Isotope shifts (measured and predicted) for PCU triol **3**.

Hydroxyl group	Experimental isotope shift (ppb)	Predicted shift using additivity (ppb)
C ₁ OH _b (mono)	-27.4	
C ₁ OH _c (mono)	+2.3	
C ₁ OH _d (di)	-24.6	-25.1 (b+c)
C ₃ OH _b (mono)	+4.0	
C ₃ OH _c (mono)	-30.8	
C ₃ OH _d (di)	-27.1	-26.8 (b+c)
C ₆ OH _b (mono)	+3.7	
C ₆ OH _c (mono)	-25.9	
C ₆ OH _d (di)	-22.3	-22.2 (b+c)

We next examined the OH/OH/OH/OH system of inositol-derived tetrol **2** in DMSO-*d*₆ (Figure 8). While only two hydroxyl resonances are present in the unperturbed ¹H NMR spectrum of tetrol **2**, deuteration of the parent compound is predicted to yield up to eight ¹H resonances for each hydroxyl group (OH_{a-h}). We note that the spectra would be even more complex for a tetrol lacking a plane of symmetry. In any case, we felt that this system offered a reasonably challenging test for our assignment procedure.

Upon dissolution in DMSO-*d*₆, tetrol **2** exhibited two singlet OH resonances, as expected. The low field OH resonance was again preliminarily assigned to the inner C_{3/3'}-OH groups. Upon titration with CD₃OD, a complex pattern emerged for each hydroxyl resonance (Figure 8). For the C_{3/3'}-OH groups,

this pattern developed into seven distinct peaks, with the central transition broadened sufficiently to suggest two overlapping signals. On the other hand, the C_{1/1'}-OH groups exhibited a spectrum consisting of eight well-resolved resonances. We were excited to see this result, because it suggested that a 400 MHz ¹H experiment could detect nearly all of the peaks corresponding to a tetrol-derived set of isotopologs and isotopomers.

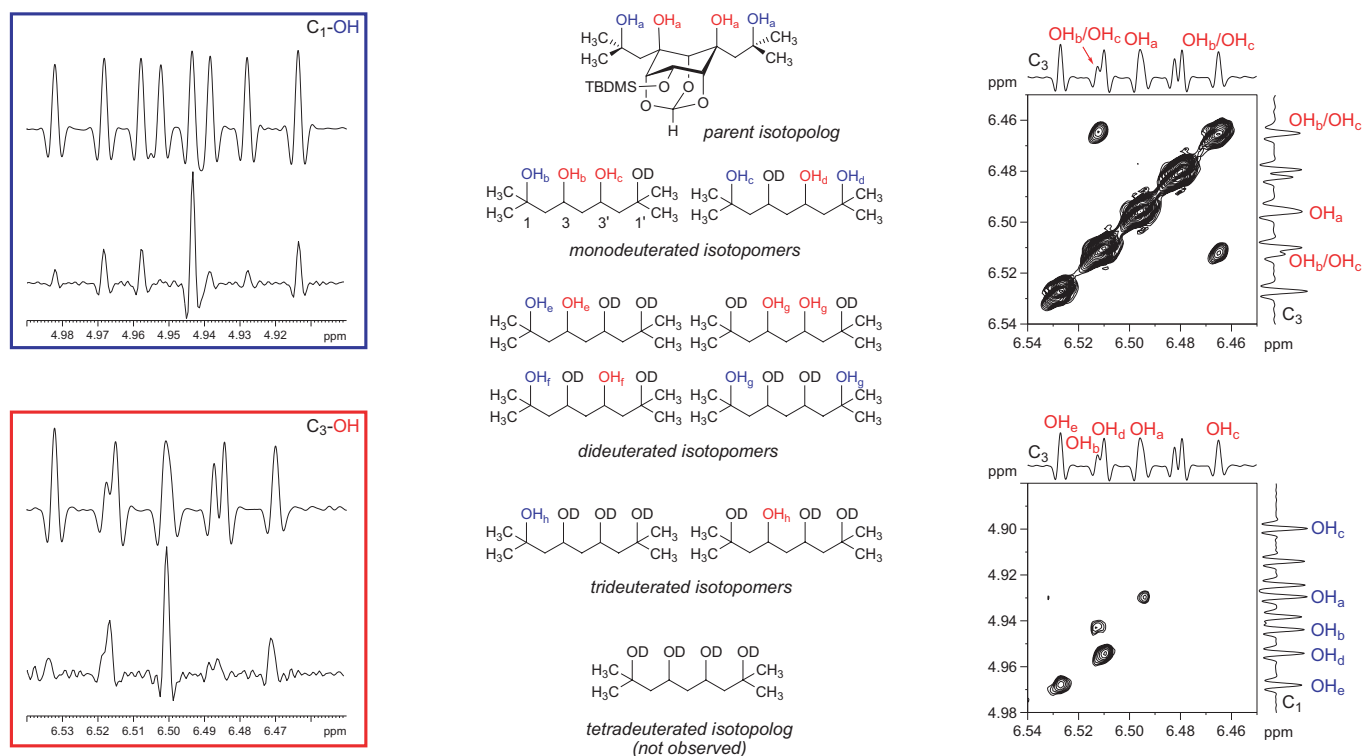


Figure 8. Left: Isotope shift perturbation of tetrol **2**. 400 MHz ¹H NMR spectra are shown for each of the two hydroxyl resonances with isotope shifts after partial deuteration of the sample. The upper traces were recorded with an increased amount of deuterium in solution. Center: labeling scheme for partially deuterated species. Right: 2D COSYLR spectra for the partially deuterated tetrol **2** with isotope assignments (200 ms delay). The region corresponding to C₃-OH/C₃-OH coupling appears above and that corresponding to C₃-OH/C₁-OH is shown below.

The 2D COSYLR spectrum of the partially deuterated compound was again used to aid in the shift assignments (Figure 8). *J*-coupling between two central hydroxyl groups is possible in only one of the isotopically labeled species, a monodeuterated isotopomer containing C₃-OH_b and C_{3'}-OH_c. Relative to the parent isotopomer, the symmetry of this molecule is reduced by the presence of deuterium at one of the terminal C₁-hydroxyl groups. As such, the internal C_{3/3'}-OH_{b/c} groups are rendered diastereotopic and potentially anisochronous. In a high-resolution 2D COSYLR experiment centered on the C₃-OH resonances, only one off-diagonal peak is observed, which allowed two of the multiplet peaks to be assigned as either C₃-OH_b or C_{3'}-OH_c. This experiment demonstrates the resolving power of the 2D COSYLR experiment, as the C_{3/3'}-OH_{b/c} shift separation in this system is only 47 ppb, or 18.8 Hz on a

400 MHz spectrometer. As shown in Figure 8, it was even possible to make an assignment of $C_{3/3}$ - $OH_{b/c}$ to the low field resonance of two overlapping peaks separated by only 0.9 Hz.

Table 4. Isotope shifts (measured and predicted) for inositol-derived tetrol **2**.

Hydroxyl group		Experimental isotope shift (ppb)	Predicted shift using additivity (ppb)
C_1	OH_b (mono)	+14.3	
C_1	OH_c (mono)	-29.8	
C_1	OH_d (mono)	+24.7	
C_1	OH_e (di)	+38.5	+39.0 (b+d)
C_1	OH_f (di)	-15.4	-15.5 (b+c)
C_1	OH_g (di)	-5.1	-5.1 (c+d)
C_1	OH_h (tri)	+8.8	+9.2 (b+c+d)
C_3	OH_b (mono)	+16.5	
C_3	OH_c (mono)	-30.7	
C_3	OH_d (mono)	+14.2	
C_3	OH_e (di)	+31.3	+30.7 (b+d)
C_3	OH_f (di)	-16.4	-16.5 (c+d)
C_3	OH_g (di)	-13.6	-14.2 (b+c)
C_3	OH_h (tri)	0	0 (b+c+d)

The C_3 - OH/C_1 - OH region of a 2D COSYLR spectrum was then used to distinguish C_3 - OH_b from C_3 - OH_c , as only C_3 - OH_b should experience coupling to an exterior hydroxyl proton. In this case, the low field resonance assigned as $C_{3/3}$ - $OH_{b/c}$ showed a correlation with an exterior OH group, identifying it as C_3 - OH_b . Three additional cross-peaks are also present in the C_3 - OH/C_1 - OH region of the COSYLR spectrum. One cross-peak arises from the parent isotopolog, while the other two cross-peaks could be combined with peak intensity data to assign C_3 - OH_d , C_3 - OH_e , C_1 - OH_d , and C_1 - OH_e . Additivity and peak intensity data was then used to assign the remaining resonances (Table 4). In this way, all sixteen hydroxyl resonances for **2** could be assigned unambiguously.

SIMPLE NMR and 2D COSYLR analysis were also performed on symmetric PCU tetrol **4** in DMSO- d_6 . In this case, assignment of the hydroxyl resonances was more challenging due to signal overlap. Rather than observing eight resonances each for the interior and exterior OH groups, only a fraction of these was clearly resolved (Figure 9). In the case of the internal C_3 - OH , only 4 resonances could be clearly observed, while for the external C_1 - OH , two groupings of three peaks each were clearly visible. We

found that a slightly elevated temperature provided better resolution of the peaks in question, and the isotope shift studies for tetrol **4** were conducted in DMSO-*d*₆ at 40 °C.

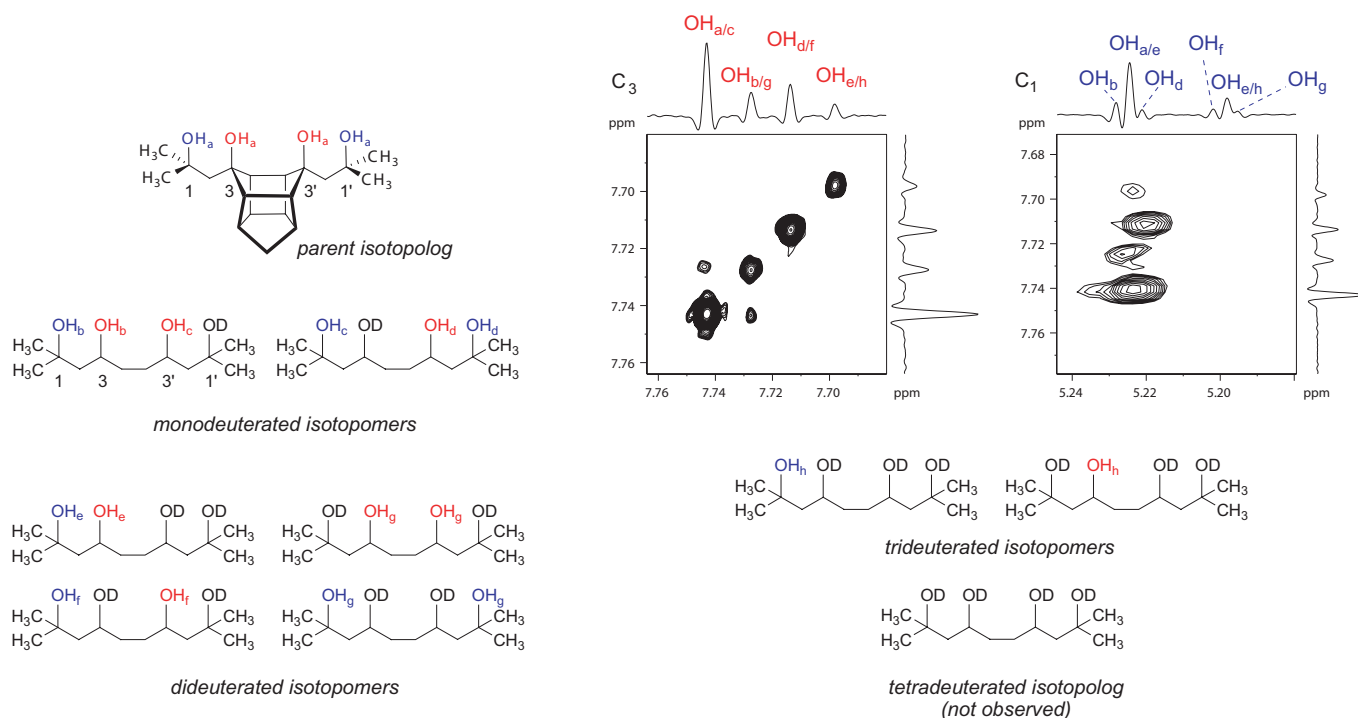
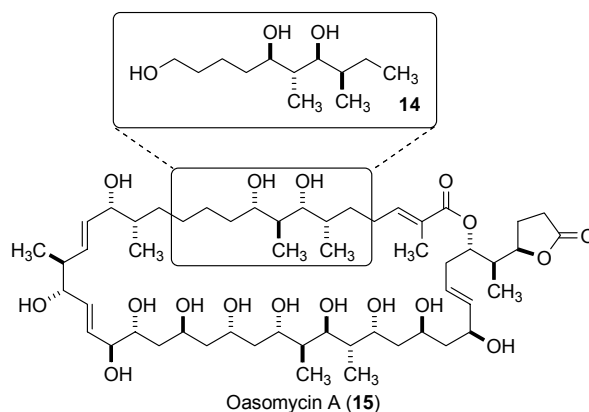


Figure 9. Isotopic perturbation of PCU tetrol **4** recorded at 40 °C in DMSO-*d*₆. Left: C_{1/1'} and C_{3/3'} hydroxyl definitions for isotopically substituted species. Right: 400 MHz ¹H 2D COSYLR spectra for partially deuterated tetrol **4**, with hydroxyl resonance assignments. Left spectrum: region corresponding to the C₃-OH hydroxyl group. The single off-diagonal correlation is evidence for C₃-OH_a/OH_b scalar coupling. Right spectrum: region showing C₃-OH/C₁-OH coupling partners.

The analysis of tetrol **4** employed a strategy very similar to that used for inositol tetrol **2**. The C₃-OH/C₃-OH region of the 2D COSYLR spectrum of tetrol **2** again revealed a single off-diagonal peak, placing either C₃-OH_b or C₃-OH_c at a position coincidental to the parent hydroxyl resonance (Figure 9). We note that this particular 2D COSYLR experiment was capable of detecting a correlation between two diagonal peaks separated by only 15.6 ppb, or 6.2 Hz on a 400 MHz spectrometer. The off-diagonal C₃-OH/C₁-OH region contained four cross-peaks, with each linking the four C₃-OH resonances to the downfield set of C₁-OH resonances. This type of pattern requires that the upfield set of C₁-OH resonances are proximal to OD groups. The most intense of these is therefore assigned as C₁-OH_c on the basis of its titration behavior. The remaining peaks in this high field C₁-OH cluster were assigned as C₁-OH_f, C₁-OH_g, and C₁-OH_h on the basis of additivity. A combination of spin-spin coupling and additivity was then used to assign the remaining C₃-OH and C₁-OH peaks. The assignments are listed in Table 5.

Table 5. Isotope shifts (measured and predicted) for PCU-derived triol **4** in DMSO-*d*₆ at 40 °C.

Hydroxyl group	Experimental isotope shift (ppb)	Predicted shift using additivity (ppb)
C ₁ OH _b (mono)	+3.7	
C ₁ OH _c (mono)	-26.3	
C ₁ OH _d (mono)	-3.3	
C ₁ OH _e (di)	0	+0.4 (b+d)
C ₁ OH _f (di)	-22.6	-22.6 (b+c)
C ₁ OH _g (di)	-33.3	-29.6 (c+d)
C ₁ OH _h (tri)	-26.3	-25.9 (b+c+d)
C ₃ OH _b (mono)	-15.6	
C ₃ OH _c (mono)	0	
C ₃ OH _d (mono)	-29.3	
C ₃ OH _e (di)	-44.9	-44.9 (b+d)
C ₃ OH _f (di)	-29.3	-29.3 (c+d)
C ₃ OH _g (di)	-15.6	-15.6 (b+c)
C ₃ OH _h (tri)	-44.9	-44.9 (b+c+d)

**Figure 10.** Oasomycin A (**15**) and acyclic triol **14**.

Application of SIMPLE NMR and the additivity principle to hydrogen bonding networks in a natural product precursor. Oasomycin A (**15**) is a polypropionate macrolactone natural product (Figure 10) that served as an interesting test case for Kishi's pioneering universal database approach to making reliable stereochemical assignments in complex natural products.²⁰ Contained within the framework of macrocycle **15** is a polypropionate unit whose relative configuration is retained in acyclic triol **14**. We have studied the isotopic perturbation behavior of triol **14** in an effort to extend our studies of hydroxyl networks to acyclic systems with natural product-derived architectures.

While the rigid systems within this study as well as many carbohydrates have been evaluated by SIMPLE NMR in DMSO- d_6 , this solvent poses difficulties for acyclic 1,3-diols. Due to strong hydrogen bonds that can occur between DMSO- d_6 and the hydroxyl groups present in these flexible substrates, the total concentration of species containing intramolecular hydrogen bonds can be quite small in this solvent. Recalling the origins of these isotope shifts (Figure 2), an intramolecular hydrogen bond is a prerequisite for the isotope effect. We have demonstrated, in fact, that a SIMPLE effect is not observed for *syn*- and *anti*-2,4-pentanediol dissolved in DMSO- d_6 . We did, however, discover that SIMPLE-type isotope effects could be measured for highly dilute solutions of acyclic diols in CD₂Cl₂, and we used this observation to develop a new ¹H NMR method for assigning relative configuration in isolated 1,3-diol units in acyclic substrates.⁸ Large negative isotope shifts were measured for *syn* 1,3-diols (20-33 ppb), whereas smaller negative isotope shifts were observed for *anti* 1,3-diols (2-16 ppb). Highly dilute diol solutions (ca. 1 mg/mL) were required for these studies, as we observed *positive* isotope shifts for samples that were five-fold more concentrated. Aggregation was thought to cause this phenomenon, as the isotope shift sign can depend upon interactions with solute and solvent (Figure 2).

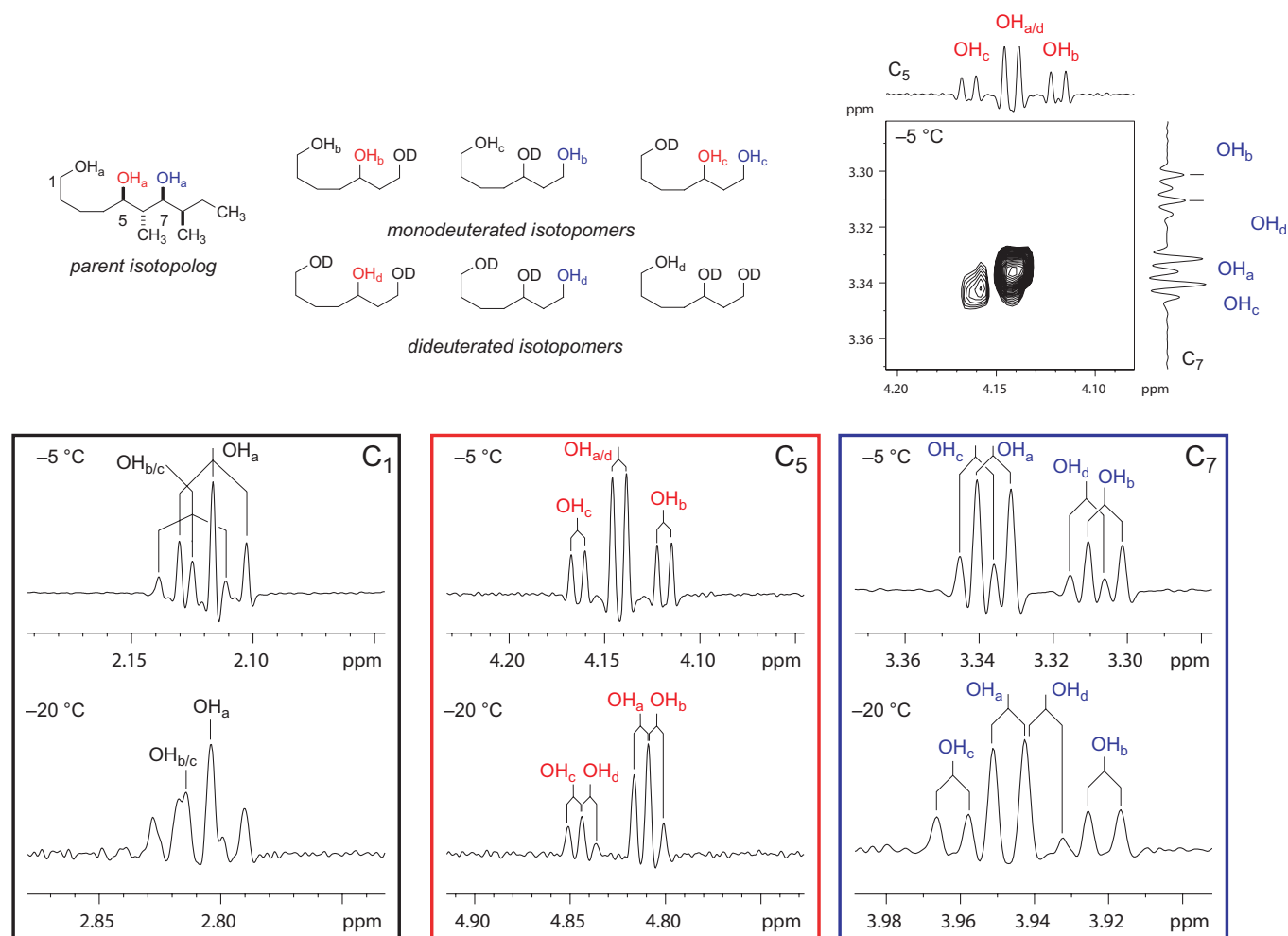


Figure 11. Labeling scheme and isotope shift perturbation of acyclic triol **14** recorded at -5 °C and -20 °C. ¹H NMR spectra were recorded for each of the three hydroxyl resonances after partial deuteration. The spectra were recorded at the same concentration and degree of deuteration.

Table 6. Isotope shifts (measured and predicted) for polypropionate **14** recorded at $-5\text{ }^{\circ}\text{C}$ and $-20\text{ }^{\circ}\text{C}$.

Hydroxyl group	Observed isotope shift at $-5\text{ }^{\circ}\text{C}$ (ppb)	Predicted shifts using additivity (ppb)	Observed isotope shift at $-20\text{ }^{\circ}\text{C}$ (ppb)	Predicted shifts using additivity (ppb)
C ₁ OH _b /OH _c	+8.4		+10.1	
C ₁ OH _b /OH _c				
C ₁ OH _d				
C ₅ OH _b	-23.7		-7.4	
C ₅ OH _c	+21.7		+34.8	
C ₅ OH _d	~0.0	-2.0 (b+c)	+27.4	+27.4 (b+c)
C ₇ OH _b	-30.1		-25.6	
C ₇ OH _c	+4.6		+15.3	
C ₇ OH _d	-25.3	-25.5 (b+c)	-10.3	-10.3 (b+c)

For triol **14** we found it necessary to perform the NMR measurements at $-5\text{ }^{\circ}\text{C}$ to shift the OH resonances into regions free of overlap. Additional data was recorded at $-20\text{ }^{\circ}\text{C}$ in order to see if the isotope shifts were temperature-dependent. As with the triols discussed earlier, dipropionate **14** was predicted to exhibit as many as four resonances per hydroxyl group upon partial deuteration, assuming that the terminal hydroxyl group was involved in an extended hydrogen bond network. This multiplicity was observed for the two secondary hydroxyl groups but not for the primary hydroxyl group, which exhibited only one new downfield resonance upon isotopic substitution (Figure 11).

Upon partial deuteration, a new downfield resonance developed for the primary C₁-OH hydroxyl group. The isotomeric identity of this resonance could not be established, as we were unable to measure any COSLYR interactions between the C₁-OH group and any of the other OH groups. Accordingly, we assign this ambiguous downfield resonance as C₁-OH_{b/c}, on the assumption that it is originating from one of the monodeuterated species. The C₁-OH isotope shift showed a modest downfield shift upon cooling from $-5\text{ }^{\circ}\text{C}$ (+8.4 ppm) to $-20\text{ }^{\circ}\text{C}$ (+10.1 ppb).

The secondary C₅-OH group exhibited isotope shifts indicative of its participation in a contiguous triol network. Namely, at $-5\text{ }^{\circ}\text{C}$ it showed a downfield (+21.7 ppb) and an upfield (-23.7 ppb) isotope shift arising from monodeuteration. The downfield resonance was assigned as C₅-OH_c on the basis of scalar

coupling to C₇-OH_c (Figure 11). Upon cooling to -20 °C, the isotopic multiplets showed pronounced temperature coefficients, as the C₅-OH_c resonance shifted to +34.8 ppb and the C₅-OH_b resonance decreased in magnitude to -7.4 ppb. The C₅-OH_b resonance, arising from the dideuterated species, became visible at +27.4 ppb, which correlated well with an additivity prediction of +27.4 ppb.

The C₇-OH resonance exhibited similar behavior upon partial deuteration of triol **14**, although the magnitude and sign of the isotope shifts were different from those observed for the C₅-OH resonance. At -5 °C, for example, four distinct resonances were observed for C₇-OH. Here again, C₇-OH_b resonated upfield (-30.1 ppb) and the C₇-OH_c resonance was observed just downfield (+4.6 ppb) of the parent C₇-OH_a resonance. At -5 °C, the isotope shift for C₇-OH_b decreased in magnitude to -25.6 ppb, whereas the isotope shift for C₇-OH_c increased to +15.3 ppb.

Several aspects of this system are discussed here. The C₅-OH isotope shifts, for example, illustrate that a 1,5-diol intramolecular hydrogen bond can exhibit a fairly large isotope shift that is opposite in sign to a *syn*-1,3-diol (+21.7 vs. -23.7 ppb for 1,5- vs 1,3-, respectively). At -5 °C, the 1,3-diol isotope shift observed for C₅-OH_b (-23.7 ppb) fell within the diagnostic value for *syn*-1,3-diols (20-33 ppb, negative). At -5 °C, this value decreased to -7.4 ppb, which is well outside the diagnostic values. The distal C₇-OH_b group, on the other hand, exhibited isotope shifts typical of a *syn*-1,3-diol at either temperature. This behavior serves to reinforce our contention that using isotope shifts to assign 1,3-diol relative configuration is predicated on the assumption that the diol fragment is isolated from other hydrogen bonding interactions.⁸

CONCLUSIONS

These studies have combined synthesis, X-ray crystallography, isotopic perturbation and 2D COSYLR spectroscopy to provide new insights regarding the use of SIMPLE NMR for detecting contiguous networks of OH...OH hydrogen bonds, including confirmation that the isotope effects in these systems are additive. We have shown that it is possible to employ additivity, signal intensity, and hydrogen bond mediated *J*-couplings to completely assign the hydroxyl region in isotopically perturbed spectra. In DMSO-*d*₆ solution, these isotope shifts are likely to be best used as qualitative markers of the number of interacting hydroxyl groups. Our studies show that the interpretation of the magnitude and sign of the isotope shifts for any given species remains a complex issue in DMSO-*d*₆. As exemplified by the example of polypropionate triol **14**, non-hydrogen bonding solvents (e.g. CDCl₂ or benzene-*d*₆) may offer more promising solutions to understanding these complexities.

EXPERIMENTAL

General Experimental Details. All reactions were performed under a nitrogen atmosphere. THF was distilled from sodium metal. ^1H and ^{13}C NMR spectra were obtained on a Bruker Avance 400 MHz NMR spectrometer. Chemical shifts are reported in ppm relative to CHCl_3 or benzene- d_5 . Multiplicity is indicated as follows: s (singlet); d (doublet); t (triplet); q (quartet); m (multiplet); dd (doublet of doublets); dt (doublet of triplets), app (apparent). IR spectra were obtained on a Perkin-Elmer 1600 Series FT-IR.

Preparation of Methyl Triol 1a. Ester **5**⁶ (803 mg, 1.59 mmol) was dissolved in THF (8 mL) and cooled to 0 °C in an ice bath. Methylmagnesium chloride (5.3 mL, 15.9 mmol, 3.0 M in THF) was added dropwise via syringe, and the reaction mixture was stirred under an argon atmosphere for 10 min at 0 °C before being brought to rt for approximately 2 h. The reaction was then diluted with Et_2O (100 mL) and quenched with the addition of saturated aqueous NH_4Cl solution (50 mL). The organic layer was separated, washed with brine, and dried over sodium sulfate. Evaporation of solvent gave a residue which was purified by silica gel column chromatography (1.25 × 8 in, 8:1 to 4:1 $\text{CH}_2\text{Cl}_2/\text{EtOAc}$) to yield 508 mg (84.8%) of triol **1a** as a white solid: mp 111.0–112.9 °C; ^1H NMR (400 MHz, C_6D_6) δ 6.46 (s, 1H), 5.70 (d, $J = 0.9$ Hz, 1H), 4.88 (d, $J = 6.3$ Hz, 1H), 4.78 (dt, $J = 6.3, 2.5$ Hz, 1H), 4.72–4.74 (m, 1H), 4.44–4.47 (m, 1H), 4.22–4.26 (m, 2H), 2.24 (d, $J = 10.2$ Hz, 1H), 2.15 (d, $J = 10.2$ Hz, 1H), 2.02 (s, 1H), 1.15 (s, 9H), 1.08 (s, 3H), 1.07 (s, 3H), 0.291 (s, 3H), 0.288 (s, 3H); ^{13}C NMR (100 MHz, C_6D_6) δ 103.3, 78.9, 75.3, 74.3, 73.5, 73.2, 69.6, 62.2, 44.9, 31.4, 26.3, 18.7, -4.27, -4.34; IR (film) ν 3342, 2943, 2861, 1255, 1161, 1002, 838 cm^{-1} ; HRMS (EI) m/z 376.1915 [376.1917 calcd for $\text{C}_{17}\text{H}_{32}\text{O}_7\text{Si}$ (M+H)].

Preparation of Benzyl Triol 1b. To ester **6**⁶ (40 mg, 0.1 mmol) in THF (0.2 mL) was added benzylmagnesium chloride (2.0 M in THF, 0.77 mL, 1.54 mmol). The mixture was then maintained for 24 h before adding EtOAc (5 mL), saturated aqueous NH_4Cl (5 mL), and H_2O (5 mL). The phases were separated, and the aqueous phase was extracted with EtOAc (2 × 5 mL). The combined organic phases were washed with brine (5 mL), dried (Na_2SO_4), and concentrated *in vacuo*. Purification by column chromatography (3:1 hexanes/EtOAc) afforded 33 mg (61%) of triol **1b** as a white foamy solid: mp 43.1–46.1 °C; ^1H NMR (400 MHz, C_6D_6) δ 7.13–7.27 (m, 6H), 6.99–7.09 (m, 4H), 5.73 (s, 1H), 5.56 (s, 1H), 4.67–4.74 (m, 2H), 4.42–4.46 (m, 1H), 4.33 (q, $J = 1.9$ Hz, 1H), 4.27 (d, $J = 9.7$ Hz, 1H), 4.14–4.17 (m, 1H), 2.91 (d, $J = 13.8$ Hz, 1H), 2.83 (d, $J = 13.8$ Hz, 1H), 2.65 (d, $J = 13.5$ Hz, 2H), 2.40 (s, 2H), 1.74 (s, 1H), 1.12 (s, 9H), 0.25 (s, 3H), 0.24 (s, 3H); ^{13}C NMR (100 MHz, C_6D_6) δ 136.6, 136.5, 131.33, 131.27, 128.8, 127.7, 127.3, 127.2, 103.3, 78.7, 76.6, 75.2, 74.2, 73.2, 69.5, 62.2, 47.4, 47.1, 41.0, 26.2, 18.6, -4.36, -4.44; IR (thin film) 3370 (broad), 3061, 2953, 2929, 2856, 1471, 1165 cm^{-1} ; HRMS (FAB+) m/z 529.2602 [529.2622 calcd for $\text{C}_{29}\text{H}_{41}\text{O}_7\text{Si}$ (M+H)].

Preparation of Phenyl Triol 1c. To ester **6**⁶ (40 mg, 0.1 mmol) in THF (0.1 mL) was added phenylmagnesium chloride (2.0 M in THF, 0.62 mL, 1.23 mmol). The mixture was then warmed to reflux for 6 h before cooling to rt and adding EtOAc (5 mL), saturated aqueous NH₄Cl (5 mL), and H₂O (5 mL). The phases were separated, and the aqueous phase was extracted with EtOAc (2 x 5 mL). The combined organic phases were washed with brine (5 mL), dried (Na₂SO₄), filtered, and concentrated *in vacuo*. Isolation of the product as a mixture with the monoalkylated phenyl ketone (~7:1) was achieved via column chromatography (3:1 hexanes/EtOAc).

To the mixture of triol **1c** and ketone (~7:1) in THF (0.1 mL) was added phenylmagnesium chloride (2.0 M in THF, 0.48 mL, 0.96 mmol). The mixture was then warmed to reflux for 6 h before cooling to rt and adding EtOAc (5 mL), saturated aqueous NH₄Cl (5 mL), and H₂O (5 mL). The phases were separated and the aqueous phase was extracted with EtOAc (2 x 5 mL). The combined organic phases were washed with brine (5 mL), dried (Na₂SO₄), filtered, and concentrated *in vacuo*. Purification by column chromatography (3:1 hexanes/EtOAc) afforded 46 mg (89% from ester **6**) of triol **1c** as a white foamy solid: mp 164.3–166.4 °C; ¹H NMR (400 MHz, C₆D₆) δ 7.38–7.43 (m, 4H), 7.15–7.22 (m, 4H), 7.06–7.14 (m, 2H), 6.25 (s, 1H), 5.68 (s, 1H), 4.49–4.55 (m, 2H), 4.26–4.31 (m, 1H), 4.12 (d, *J* = 9.2 Hz, 1H), 3.66–3.69 (m, 1H), 3.58–3.63 (m, 1H), 3.10 (AB q, *J* = 15.9 Hz, 2H), 2.76 (s, 1H), 1.10 (s, 9H), 0.19 (s, 3H), 0.18 (s, 3H); ¹³C NMR (100 MHz, C₆D₆) δ 146.8, 146.5, 126.21, 126.19, 103.2, 79.9, 77.9, 75.2, 74.8, 72.8, 69.5, 62.0, 43.6, 26.3, 18.7, –4.39, –4.44; IR (thin film) 3319 (broad), 2953, 2929, 2856, 1448, 1164 cm⁻¹; HRMS (FAB+) *m/z* 501.2320 [501.2309 calcd for C₂₇H₃₇O₇Si (M+H)].

Preparation of Ester 8. Pyridine (4.29 mL, 53.0 mmol) was added to a solution of Dess-Martin periodinane (2.66 g, 6.14 mmol) in CH₂Cl₂ (50 mL), and the resulting solution was allowed to stir at rt under an argon atmosphere for 10 min. Triol derivative **1** (1.07 g, 2.85 mmol) was then added in portions, and the reaction was maintained at rt for 3 h. The reaction was then diluted with Et₂O (150 mL) and quenched with a 1:1 solution of saturated aqueous NaHCO₃ and saturated aqueous NaHSO₃ (50 mL). The organic layer was separated, washed twice with saturated aqueous NaHCO₃ and brine, and dried over sodium sulfate. Evaporation of solvent yielded ketone **7** as an oily residue (1.15 g, 3.07 mmol) of sufficient purity, as judged by ¹H NMR spectroscopy, for the subsequent reaction.

Ketone **7** (1.15 g, 3.07 mmol) was azeotropically dried with benzene twice and dissolved in THF (10 mL) in a conical flask under argon. Lithio ethyl acetate was prepared in a separate flask by adding anhydrous EtOAc (1.5 mL) dropwise to a stirred solution at -78 °C of lithium bis(trimethylsilyl)amide (1.0 M in THF, 15.4 mL, 15.4 mmol). After 15 min, the solution of ketone **7** was added dropwise via cannula. The reaction mixture was maintained at -78 °C for 20 h, after which it was diluted with Et₂O (100 mL) and quenched by the addition of saturated aqueous NH₄Cl (40 mL). The organic layer was separated, washed with brine, and dried (Na₂SO₄). Evaporation of solvent gave a residue which was purified by

silica gel column chromatography (9:1→8:1 CH₂Cl₂/EtOAc) to yield 1.07 g (81%) of triol **8** as a thick oil: ¹H NMR (400 MHz, C₆D₆) δ 6.63 (s, 1H), 5.87 (d, *J* = 0.4 Hz, 1H), 5.63 (d, *J* = 0.8 Hz, 1H), 4.80–4.83 (m, 1H), 4.71 (t, *J* = 1.3 Hz, 1H), 4.38 (q, *J* = 1.3 Hz, 1H), 4.27 (q, *J* = 1.3 Hz, 1H), 4.00–4.13 (m, 2H), 3.41 (dd, *J* = 10.2, 0.6 Hz, 1H), 3.12 (d, *J* = 10.2 Hz, 1H), 2.33 (d, *J* = 10.2 Hz, 1H), 2.24 (d, *J* = 10.2 Hz, 1H), 2.15 (s, 1H), 1.152 (s, 9H), 1.148 (3H, s), 1.20 (s, 3H), 1.05 (t, *J* = 4.8 Hz, 3H), 0.30 (s, 6H); ¹³C NMR (100 MHz, C₆D₆) δ 171.9, 103.2, 78.3, 77.9, 74.7, 74.1, 73.2, 72.2, 62.7, 60.7, 45.1, 41.00, 31.5, 31.4, 26.3, 18.7, 14.3, -4.3, -4.4; IR (thin film) 3397, 2957, 2932, 2857, 1734, 1163 cm⁻¹; HRMS (MALDI) *m/z* 485.2184 [485.2177 calcd for C₂₁H₃₈O₉SiNa (M+Na)].

Preparation of Tetrol 2. Ester triol **8** (794 mg, 1.72 mmol) was dissolved in THF (15 mL) and cooled to 0 °C in an ice bath. Methylmagnesium bromide (5.7 mL, 17 mmol, 3.0 M in Et₂O) was added dropwise via syringe, and the reaction mixture was maintained under an argon atmosphere for 10 min at 0 °C before warming to rt and maintained at that temperature for approximately 3.5 h. The reaction was then diluted with Et₂O (85 mL) and quenched with saturated aqueous NH₄Cl (35 mL). The organic layer was separated, washed with brine, and dried over sodium sulfate. Evaporation of the solvent gave a residue which was purified by silica gel column chromatography (1.25 × 8 in, 4:1 to 2:1 CH₂Cl₂/EtOAc) to yield 528 mg (69%) of tetrol **2** as a white solid: mp 118.3–119.6 °C; ¹H NMR (400 MHz, C₆D₆) δ 6.82 (s, 2H), 5.63 (d, *J* = 0.8 Hz, 1H), 4.75–4.78 (m, 1H), 4.34 (t, *J* = 1.2 Hz, 1H), 4.29 (t, *J* = 1.3 Hz, 2H), 4.03 (s, 2H), 2.44 (d, *J* = 10.1 Hz, 2H), 2.34 (d, *J* = 10.1 Hz, 2H), 1.35 (s, 12H), 1.17 (s, 9H), 0.31 (s, 6H); ¹³C NMR (100 MHz, C₆D₆) δ 103.1, 78.3, 76.3, 74.5, 72.8, 62.6, 45.7, 31.7, 31.6, 26.3, 18.7, -4.3; IR (thin film) 3301, 2957, 2930, 2858, 1165 cm⁻¹; HRMS (EI) 448.2494 [448.2492 calcd for C₂₁H₄₀O₈Si (M+H)].

Preparation of 2-methylallylmagnesium chloride. A 3-necked flask was charged with magnesium turnings (9.7 g, 400 mmol), THF (80 mL), and I₂ (one crystal) and warmed to 50 °C. Approximately 10 mL of a solution of 3-chloro-2-methylpropene (15.6 mL, 160 mmol) freshly distilled from CaCl₂ in THF (20 mL) was then added over 2 min to promote initiation as indicated by the rapid evolution of gas and loss of color. (Note: initiation can take up to 20 min to occur after the chloride is added.) Upon initiation, the remaining chloride solution was added at a rate sufficient to maintain reflux. The reaction was then warmed to reflux and maintained for 2 h before cooling to rt. The liquid phase of the reaction was then transferred via canula to a flask equipped with a 3-way adapter for storage. The excess magnesium was recovered and weighed in order to determine the approximate molarity of the 2-methylallylmagnesium chloride solution. The reagent was used directly in further transformations.

Preparation of Alkene 10. Benzyl ketone **9** (112 mg, 0.42 mmol) was azeotroped from benzene and then dissolved in THF (3.0 mL) and cooled to -78 °C. 2-Methylallylmagnesium chloride (0.96 M in THF, 3.29 mL, 3.16 mmol) was added dropwise. After 4 h, EtOAc (4 mL), saturated aqueous NH₄Cl (5

mL) and H₂O (5 mL) were added. The phases were separated, and the aqueous phase was extracted with EtOAc (2 x 10 mL). The combined organic layers were washed with brine (10 mL), dried (Na₂SO₄), and concentrated *in vacuo*. Purification by column chromatography (19:1 hexanes/EtOAc) gave 131 mg (97%) of alkene **10** as a white solid: mp 74.2–75.2 °C; ¹H NMR (400 MHz, CDCl₃) δ 7.29–7.39 (m, 5H), 6.40 (s, 1H), 4.85–4.88 (m, 1H), 4.72 (app s, 1H), 4.62 (AB q, *J* = 17.8, 11.9 Hz, 2H), 3.64 (t, *J* = 3.4 Hz, 1H), 2.82–2.87 (m, 1H), 2.47–2.58 (m, 5H), 2.28–2.31 (m, 1H), 2.17–2.22 (m, 2H), 2.03 (dd, *J* = 13.8, 1.8 Hz, 1H), 1.92 (s, 3H), 1.63 (d, *J* = 10.7 Hz, 1H), 1.11 (d, *J* = 10.7 Hz, 1H); ¹³C NMR (100 MHz, CDCl₃) δ 143.9, 137.0, 128.5, 127.9, 127.7, 113.1, 79.1, 77.5, 71.9, 48.6, 46.6, 44.3, 43.8, 43.7, 43.1, 43.5, 38.2, 35.6, 34.4, 24.6; IR (thin film) 3359, 2954, 1640, 1431, 1275 cm⁻¹; HRMS (FAB+) *m/z* 323.2007 [323.2011 calcd for C₂₂H₂₇O₂ (M+H)].

Preparation of Diol 11. To Hg(OAc)₂ (99 mg, 0.31 mmol) were added H₂O (0.4 mL) and THF (0.4 mL), resulting in the formation of a bright yellow color. After 15 min, alkene **10** (100 mg, 0.31 mmol) was added and the color dissipated. After 1 h, aqueous NaOH (3M, 0.4 mL) was added followed by a solution of NaBH₄ (6 mg, 0.16 mmol) in aqueous NaOH (3M, 0.4 mL). The resulting solution appeared black in color. The reaction was maintained for 3 h before transferring to a separatory funnel. The mercury was allowed to settle over 18 h before removal from the separatory funnel. The remaining reaction mixture was extracted with EtOAc (3 x 20 mL). The combined organic phases were then washed with brine (20 mL), dried (Na₂SO₄), and concentrated *in vacuo*. Purification by column chromatography (9:1 hexanes/EtOAc) afforded 94 mg (89%) of diol **11** as a thick colorless oil: ¹H NMR (400 MHz, CDCl₃) δ 7.30–7.41 (m, 5H), 6.98 (s, 1H), 5.43 (broad s, 1H), 4.61 (AB q, *J* = 13.0, 11.7 Hz, 2H), 3.66 (t, *J* = 3.3 Hz, 1H), 2.80–2.85 (m, 1H), 2.71–2.75 (m, 1H), 2.52–2.57 (m, 3H), 2.41 (app s, 1H), 2.31 (app s, 1H), 2.22–2.27 (m, 1H), 1.60–1.66 (m, 2H), 1.47 (dd, *J* = 14.5, 1.0 Hz, 1H), 1.32 (s, 3H), 1.25 (s, 3H), 1.13 (d, *J* = 10.7 Hz, 1H); ¹³C NMR (100 MHz, CDCl₃) δ 136.6, 128.6, 128.1, 127.9, 79.0, 78.8, 72.2, 71.1, 52.2, 48.9, 43.8, 43.7, 43.2, 42.9, 40.4, 38.0, 35.7, 34.3, 31.7, 30.5; IR (thin film) 3282, 2965, 1440, 1268, 1153, 1072 cm⁻¹; HRMS (MALDI) *m/z* 363.1922 [363.1931 calcd for C₂₂H₂₈O₃Na (M+Na)].

Preparation of Triol 3. To a solution of diol **11** (93 mg, 0.27 mmol) in EtOAc (20 mL) was added 10% Pd/C (14 mg, 15% wt/wt). The reaction was purged with nitrogen and then placed under a hydrogen atmosphere. After 40 min, the reaction was filtered through Celite and concentrated *in vacuo*. Purification by column chromatography (1:1 hexanes/EtOAc) gave 64 mg (94%) of triol **3** as a white solid: mp 109.5–111.7 °C; ¹H NMR (400 MHz, CDCl₃) δ 5.82 (broad s, 2H), 3.79 (s, 1H), 2.66–2.70 (m, 2H), 2.52 (app s, 2 H), 2.25–2.44 (m, 4H), 1.62 (AB d, *J* = 14.7 Hz, 1H), 1.61 (d, *J* = 10.4 Hz, 1H), 1.53 (AB d, *J* = 14.7 Hz, 1H), 1.34 (s, 3H), 1.31 (s, 3H), 1.08 (d, *J* = 10.6 Hz, 1H); ¹³C NMR (100 MHz, CDCl₃) δ 79.1, 72.5, 71.5, 51.6, 48.3, 46.7, 43.9, 43.4, 43.1, 40.1, 38.6, 38.5, 34.3, 31.8, 31.0; IR (thin

film) 3164, 2965, 1475, 1263, 1155 cm^{-1} ; HRMS (MALDI) m/z 273.1460 [273.1461 calcd for $\text{C}_{15}\text{H}_{22}\text{O}_3\text{Na}$ (M+Na)].

Preparation of Diene 13. To a solution of pentacyclo-[5.4.0.02,6.03,10.05,9]undecane-8,11-dione (**12**, 744 mg, 4.27 mmol) in THF (15 mL) was added 2-methylallylmagnesium chloride (0.96 M, 44.5 mL, 42.7 mmol) dropwise. The reaction was then warmed to reflux for 3 h before being cooled to rt. EtOAc (20 mL), saturated aqueous NH_4Cl (20 mL) and H_2O (20 mL) were added, and the phases were separated. The aqueous phase was extracted with EtOAc (40 mL). The combined organic phases were then washed with brine (40 mL), dried (Na_2SO_4) and concentrated *in vacuo* to yield 1.20 g (98%) of diene **13** as a white solid: mp 148.2–151.9 °C; ^1H NMR (400 MHz, CDCl_3) δ 5.54 (broad s, 2H), 4.92–4.96 (m, 2H), 4.79 (app s, 2H), 2.47–2.60 (m, 6H), 2.21 (app s, 2H), 2.16 (d, $J = 9.1$ Hz, 4H), 1.89 (s, 6H), 1.57 (d, $J = 10.0$ Hz, 1H), 1.12 (d, $J = 10.7$ Hz, 1H); ^{13}C NMR (100 MHz, CDCl_3) δ 143.1, 114.7, 77.2, 50.0, 47.2, 44.5, 43.6, 39.6, 34.0, 24.8; IR (thin film) 3151, 2949, 1639, 1448, 1280 cm^{-1} ; HRMS (MALDI) m/z 309.1841 [309.1825 calcd for $\text{C}_{19}\text{H}_{26}\text{O}_2\text{Na}$ (M+Na)].

Preparation of Tetrol 4. To $\text{Hg}(\text{OAc})_2$ (1.12 g, 3.5 mmol) were added H_2O (2 mL) and THF (2 mL) resulting in the formation of a bright yellow color. After 20 min, diene **13** (500 mg, 1.75 mmol) was added and the color dissipated. After 1 h, aqueous NaOH (3M, 2 mL) was added followed by a solution of NaBH_4 (66 mg, 1.75 mmol) in aqueous NaOH (3M, 2 mL). The resulting solution appeared black in color. The reaction was maintained for 3 h before transferring to centrifuge tube. The reaction was spun down for 5 min after which the liquid was transferred to a separatory funnel. After removing the organic phase, the aqueous phase was extracted with EtOAc (3 x 50 mL). The combined organic phases were then washed with brine (50 mL), dried (Na_2SO_4), and concentrated *in vacuo*. Purification by column chromatography (2:1→1:1→1:2 hexanes/EtOAc) afforded 351 mg (62%) of tetrol **4** as a white solid: mp 135.9–138.3 °C; ^1H NMR (400 MHz, CDCl_3) δ 7.53 (broad s, 2H), 4.39 (broad s, 2H), 2.68 (d, $J = 5.0$ Hz, 2H), 2.50–2.52 (m, 2H), 2.39 (app s, 2H), 2.32 (app s, 2H), 1.66 (AB d, $J = 14.7$ Hz, 2H), 1.56 (d, $J = 10.0$ Hz, 1H), 1.55 (AB d, $J = 14.7$ Hz, 2H), 1.35 (s, 6H), 1.32 (s, 6H), 1.11 (d, $J = 10.7$ Hz, 1H); ^{13}C NMR (100 MHz, CDCl_3) δ 78.7, 72.6, 53.0, 48.5, 44.1, 43.6, 39.2, 34.1, 31.9, 31.2; IR (thin film) 3149, 2968, 1481, 1175 cm^{-1} ; HRMS (MALDI) m/z 345.2050 [345.2036 calcd for $\text{C}_{19}\text{H}_{30}\text{O}_4\text{Na}$ (M+Na)].

NMR Measurements. NMR spectra were recorded at rt (19 °C), unless otherwise specified on a Bruker Avance 400 MHz NMR spectrometer. Acquisition parameters: 16 scans, 4195 Hz sweep width, 32K file size, 0.128 Hz/pt digital resolution. Processing parameters: in certain cases, Gaussian resolution enhancement was applied in order to resolve very small (<2 ppb) isotope shifts. Isotope shifts were obtained via the resident spectrometer software peak-picking algorithm, which takes the observed maximum point and fits a parabola through it and its two nearest neighbors. Using the acquisition

parameters described above, we estimate the uncertainty in any given measurement to be ± 0.1 ppb or ± 0.04 Hz at 400 MHz. This estimation was obtained by performing a statistical analysis of the peak-to-peak separation within the five-line ^1H multiplet arising from the trace amount of DMSO- d_5 . Partial deuteration of hydroxyl groups accomplished by careful addition of microliter aliquots of CD_3OD to an NMR tube containing the compound (ca. 1 mg) dissolved in deuterated DMSO or methylene chloride (800 μL).

ACKNOWLEDGMENT

This work was supported by the National Science Foundation, the Camille and Henry Dreyfus Foundation, and Pomona College. We thank Dr. Saeed Khan of the UCLA Department of Chemistry and Biochemistry for assistance with X-ray crystallography. The authors dedicate this paper to Professor Yoshito Kishi on the occasion of his 70th birthday.

REFERENCES AND NOTES

1. G. A. Jeffrey and W. Saenger, *Hydrogen Bonding in Biological Structures*; Springer-Verlag: New York, 1991.
2. (a) Y. Huang, A. K. Unni, A. N. Thadani, and V. H. Rawal, *Nature*, 2003, **424**, 146. (b) B. Gerard, S. Sangji, D. J. O'Leary, and J. A. Porco, Jr., *J. Am. Chem. Soc.*, 2006, **128**, 7754.
3. For representative ^1H applications, see: (a) R. U. Lemieux and K. Bock, *Jpn. J. Antibiotics*, 1979, **32**, S163. (b) J. C. Christofides and D. B. Davies, *J. Chem. Soc., Chem. Commun.*, 1982, 560. (c) J. C. Christofides and D. B. Davies, *J. Am. Chem. Soc.*, 1983, **105**, 5099. (d) J. C. Christofides and D. B. Davies, *J. Chem. Soc., Chem. Commun.*, 1985, 1533. (e) J. C. Christofides, D. B. Davies, J. A. Martin, and E. B. Rathbone, *J. Am. Chem. Soc.*, 1986, **108**, 5738. (f) D. B. Davies and J. C. Christofides, *Carbohydr. Res.*, 1987, **163**, 269. (g) J. R. Everett, *J. Chem. Soc., Chem. Comm.*, 1987, 1878. (h) P. Uhlmann and A. Vasella, *Helv. Chim. Acta*, 1992, **75**, 1979. (i) P. E. Hansen, M. Christofferson, and S. Bolvig, *Magn. Reson. Chem.*, 1993, **31**, 893. (j) S. J. Angyal and J. C. Christofides, *J. Chem. Soc., Perkin Trans. 2*, 1996, 1485. (k) J. Dabrowski, H. Grosskurth, C. Baust, and N. E. Nifant'ev, *J. Biomol. NMR*, 1998, **12**, 161.
4. M. Saunders and M. H. Jaffe, *J. Am. Chem. Soc.*, 1971, **93**, 2558.
5. J. Reuben, *J. Am. Chem. Soc.*, 1985, **107**, 1756.
6. B. N. Craig, M. U. Janssen, B. M. Wickersham, D. M. Rabb, P. S. Chang, and D. J. O'Leary, *J. Org.*

- Chem.*, 1996, **61**, 9610.
7. T. E. Vasquez, Jr., J. M. Bergset, M. B. Fierman, A. Nelson, J. Roth, S. I. Khan, and D. J. O'Leary, *J. Am. Chem. Soc.*, 2002, **124**, 2931.
 8. C. E. Anderson, D. K. Britt, S. Sangji, D. J. O'Leary, C. D. Anderson, and S. D. Rychnovsky, *Org. Lett.*, 2005, **7**, 5721.
 9. M. B. Fierman, A. Nelson, S. I. Khan, M. Barfield, and D. J. O'Leary, *Org. Lett.*, 2000, **2**, 2077.
 10. M. Barfield, J. M. Bergset, and D. J. O'Leary, *Mag. Reson. Chem.*, 2001, **39**, S115.
 11. N. Loening, C. E. Anderson, W. S. Iskenderian, C. D. Anderson, S. D. Rychnovsky, M. Barfield, and D. J. O'Leary, *Org. Lett.*, 2006, **8**, 5321.
 12. J. C. Christofides and D. B. Davies, *J. Chem. Soc., Perkin Trans. 2*, 1987, 97.
 13. For a theoretical study of this effect in the water dimer, see: S. Scheiner and M. Cuma, *J. Am. Chem. Soc.*, 1996, **118**, 1511.
 14. G. Carr and D. Whittaker, *J. Chem. Soc., Perkin Trans. 2*, 1989, 359.
 15. The structures were solved by standard methods. The author has deposited atomic coordinates for **1a**, **2**, **3**, and **4**, and **13** with the Cambridge Crystallographic Data Centre.
 16. O. L. Chapman and R. W. King, *J. Am. Chem. Soc.*, 1964, **86**, 1256.
 17. A standard procedure was used for the determination of exchange rate constants. For a detailed description, see: D. R. Anderson, D. D. Hickstein, D. J. O'Leary, and R. H. Grubbs, *J. Am. Chem. Soc.*, 2006, **128**, 8386.
 18. B. Bernet and A. Vasella, *Helv. Chim. Acta*, 2000, **83**, 995.
 19. (a) A. Bax and R. Freeman, *J. Magn. Res.*, 1981, **44**, 542. (b) A. Bax, 'Two-Dimensional Nuclear Magnetic Resonance,' Delft University Press, Delft, 1982.
 20. Y. Kobayashi, C.-H. Hong, and Y. Kishi, *J. Am. Chem. Soc.*, 2001, **123**, 2076.